Serb. Astron. J. № 212 (2026), 31 - 46
DOI: https://doi.org/10.2298/SAJ2612031V

UDC 524.8 : 524.882 : 530.12
Original scientific paper

THE STUDY OF ANISOTROPIC BOUNCING COSMOLOGICAL MODELS IN MODIFIED GRAVITY

T. Vinutha[1], K. Niharika[2] and K. Sri Kavya[3]

[1] *Dept. of Applied Mathematics, AUCST, Andhra University, Visakhapatnam-530003, India*
E–mail: *vinuthatummala@gmail.com*

[2] *Dept. of Mathematics, Vignan's Institute of Information Technology(Autonomous), Visakhapatnam-530049, India*

[3] *Dept. of Mathematics, Maharaj Vijayaram Gajapathi Raj College of Engineering, Vizianagaram-535005, India*

(Received: July 21, 2025; Accepted: December 19, 2025)

SUMMARY: The current work aims to investigate the anisotropic Bianchi type - III, V, and VI_0 bouncing cosmological models in modified gravity. The present study deals with the examination of $f(R,T)$ gravity, i.e., $f_1(R)+f_2(T)=R-\nu\gamma\tanh(\frac{R}{\gamma})+\lambda T$ where ν, γ, λ are constants, R is the Ricci scalar, and T is the trace of the energy-momentum tensor. Two assumptions are to be considered for solving the field equations of the three models: i) the expansion scalar is proportional to the shear scalar, and ii) the bouncing scale factor. Here, the bouncing scale factor is studied in exponential form (i.e., a symmetric bounce) and, as a result, the graphs show that the contracting phase reflects the expanding phase. Some parameters of the three models are analyzed, and the graphs of those parameters are used to describe their relevance. Energy conditions are evaluated within the context of $f(R,T)$ gravity, and the results are deduced as the infringement of the null and strong energy conditions, which exhibits an accelerated universe scenario, whereas the dominant energy condition is fulfilled. The stability of the obtained model is examined using the perturbation technique. This article yielded intriguing results that support the current observations of the cosmos.

Key words. Cosmology: theory – Gravitation

1. INTRODUCTION

During the 20^{th} century, a lot of research was done in cosmology, and one of the most significant discoveries of that research was the rapid universe's expansion. As this is an exciting topic in recent times, many researchers are likely to have enthusiasm for exploring this topic. Experimental results evidence that the universe is in a state of accelerated expansion as observed from cosmic observations, such as supernova type Ia, cosmic microwave background, and large-scale structure (Riess et al. 1998, Perlmutter et al. 1999, Spergel et al. 2003, Tegmark et al. 2004). There are two possible ways to explain this rapid expansion. One of them is dark energy(DE), which is believed to arise from a form of exotic matter with negative pressure. Dark energy can be described either by the cosmological constant, or by an equation-of-state parameter defined as $\omega = \frac{p}{\rho}$, where p denotes pressure, and ρ denotes energy density. Several theoretical models have been proposed as DE candidates, including the cosmological constant, quintessence, phantom energy, tachyon fields, and Chaplygin gas models (Weinberg 1989, Peebles and Ratra 2003, Sahni and Starobinsky 2000, Caldwell 2002, Sen 2002, Kamenshchik et al. 2001). Another way is a modified version of Einstein's general relativity field equations, which can be developed by using the Einstein-Hilbert action theory.

There are numerous types of modified theories of gravity such as $f(R)$ gravity, $f(T)$ gravity, $f(G)$ gravity, $f(R,G)$ gravity, and $f(T,B)$ gravity where R, T,

G and B are Ricci scalar, Torison scalar, Gauss-Bonnet scalar, and Boundary term, respectively. Among all these theories, $f(R)$ is fascinating because of successful outcomes related to the present universe. $f(R)$ gravity can demonstrate the unification of the early-time inflation and late-time acceleration of the cosmos. The $f(R)$ theory is very important in high-energy physics for resolving the hierarchy or gravity-GUT unification issues. One of the most important phase transitions in the early universe was the one from quark-gluon plasma (QGP) to hadrons. According to the hot big bang hypothesis, such phase transitions first occurred when the universe was only a few seconds old. Dixit et al. (2023a) have discussed the cosmological consequence of the $f(R)$ dark energy scenario with the Kantowski-Sachs space-time in the context of strange quark matter with string clouds. Odintsov and Oikonomou (2025a) aim to provide a new parametrization of the power-law gravity inflation framework in the Jordan frame. Odintsov and Oikonomou (2025b) have studied confronting rainbow-deformed $f(R)$ gravity with the Atacama Cosmology Telescope (ACT) data. Nojiri et al. (2025) have explored how a dynamical oscillating and phantom crossing dark energy era can be realised in the context of $f(R)$ gravity. Nojiri et al. (2022) have discussed the integral $f(R)$ gravity and saddle point condition as a remedy for the H_0-tension. These are some of the authors who worked on various cosmological models in $f(R)$ theories of gravity. The authors who worked on $f(T)$, $f(G)$, $f(R,G)$, and $f(T,B)$ gravity are mentioned in references below. Shekh et al. (2023a) have explored observational constraints on the transit reconstructed Tsallis $f(T)$ gravity. Pradhan et al. (2024b) worked on reconstruction of the Lambda Cold Dark Matter (ΛCDM) model from $f(T)$ gravity in a viscous-fluid universe with observational constraints. Nojiri and Odintsov (2025) investigated the correspondence between modified gravity theories and the general entropic cosmology theory. Such a theory is proposed by analogy with Jacobson's work, where the Einstein equation was derived from the Bekenstein–Hawking entropy. Shekh et al. (2025) investigated a Cartesian coordinate metric viscous fluid cosmological model with interactions, using a novel parametrization of the Hubble parameter and constraining free parameters with observational data. Verma et al. (2026) have studied on Testing $f(T)$ gravity with cosmological observations: confronting the Hubble tension and implications for the late-time universe. Nojiri and Odintsov (2024) have explored Black holes, photon sphere, and cosmology in ghost-free gravity. Ghaderi et al. (2024) have constructed the Friedmann-Lemaitre-Robertson-Walker (FLRW) cosmological model of the universe by choosing the source as holographic and Renyi holographic dark energy in the context of $f(R,G)$ gravity. Shekh et al. (2023b) have studied $f(T,B)$ gravity with statistically fitting of $H(z)$.

Tsujikawa suggested one of the several $f(R)$ models which is consistent with cosmological and local gravity constraints. Among them, the feasible model is $f(R) = R - \nu\gamma\tanh(\frac{R}{\gamma})$ where ν and γ are constants. To satisfy local gravity constraints in the solar system, $f(R)$ approaches the ΛCDM model when $R >> R_0$, where R_0 is the Ricci scalar at the present epoch. Appleby and Battye (2007) proposed a model of the form $f(R) = R - \nu\gamma\tan h(\frac{R}{\gamma})$. In this model, the cosmological constant vanishes in space-time when the condition $f(R=0) = 0$ is satisfied. The derivative of $f(R)$ with respect to R is given by $1 - \nu\,\mathrm{sech}^2(\frac{R}{\gamma})$. The function $f(R) = R - \nu\gamma\tanh(\frac{R}{\gamma})$ quickly reaches $f(R) = R - \nu\gamma$ within the region $R >> \gamma$ and this model is very close to the ΛCDM model.

Tsujikawa (2008) has worked on observational signatures of the $f(R)$ dark energy models that satisfy the cosmological and local gravity constraints. Golchin and Mehdizadeh (2019) have investigated quasi-cosmological traversable wormholes in $f(R)$ gravity. De Felice and Tsujikawa (2010) have discussed the $f(R)$ theories. Amendola and Tsujikawa (2010) have studied dark energy theory and observations. Lee et al. (2011) have worked on future cosmological evolution in $f(R)$ gravity using two equations of state parameters. Liu et al. (2018) have studied constraining $f(R)$ gravity in the solar system, cosmology, and binary pulsar systems with specific $f(R)$ models (the Hu-Sawicki model, Tsujikawa model, and Starobinsky model). Inspired by the above works, in the present paper, the second form of $f(R,T)$ gravity suggested by Harko et al. (2011) is considered i.e., $f(R,T) = f_1(R) + f_2(T)$ with $f_1(R) = R - \nu\gamma\tanh(\frac{R}{\gamma})$ and $f_2(T) = \lambda T$ where ν, γ and λ are constants. In terms of energy transfer between geometry and matter, this expansion of cosmic gravity in $f(R,T)$ can be explained effectively. There are many works on linear, quadratic, exponential, and logarithmic forms of R in $f_1(R)$, but this paper is an entirely new one and, by choosing the functional form of $f(R,T) = R - \nu\gamma\tanh(\frac{R}{\gamma}) + \lambda T$, the desired solutions are obtained. In recent years, the authors who worked on various aspects of $f(R,T)$ gravity are found in references (Vinutha and Kavya 2020, Vinutha and Sri Kavya 2021, Vinutha and Venkata Vasavi 2021, Vinutha et al. 2021b, 2023, Moraes and Sahoo 2017, Sahoo et al. 2018).

Pradhan and Jaiswal (2018) have studied A class of spatially homogeneous and anisotropic Bianchi-V massive string models in the $f(R,T)$ theory of gravity in presence of magnetic field. Sharma et al. (2019) have examined the stability of the transition from the early decelerating stage of the Universe to the recent accelerating stage for the (LRS) Bianchi-I model in the $f(R,T)$ theory. Maurya et al. (2020) have investigated the Bianchi type-V cosmological models with a quark matter (QM) distribution and domain walls with observational constraints in the $f(R,T)$

theory of gravity. Dixit et al. (2023b) have studied observational constraints in a general class of Bianchi models in $f(R,T)$ gravity. Pradhan et al. (2024a) have worked on exploring wormholes in $f(R,T)$ gravity. Banerjee et al. (2025) explored quark stars in $f(R,T)$ gravity: mass-to-radius profiles, and observational data. Myrzakulov et al. (2025) worked on the $f(R,T)$ gravity theory for the flat Friedmann-Lemaitre–Robertson–Walker (FLRW) model, the accelerating expansion of the universe is investigated using a specific form of the emergent Hubble parameter.

The concept of bouncing cosmology can be traced back to the Tolman (1931) work in the 1930s, far earlier than the inflationary cosmology. Initially, the Big Bang theory discussed the universe's expansion and this theory envisaged the formation of light atomic nuclei from protons and neutrons. But, because of this theory, many problems came into existence, such as the flatness problem, horizon problem, and monopole problem. In order to solve these issues raised by the Big Bang, the cosmic inflation was needed to create a uniform, smooth, and flatness of the cosmos which was devised by Alan Guth. Despite its prominent explanation in the early universe, the inflationary cosmological model fails to illustrate the problem of singularity. Many researchers looked into this problem and devised a solution known as Big Bounce. Among various bouncing cosmological models, the physical motivation for choosing this symmetric bounce is that it does not exhibit a singularity behavior. A bouncing universe with an initial contraction to a non-vanishing minimal radius and subsequently an expanding phase provides a possible solution to the singularity problem of the standard Big Bang cosmology. Bamba et al. (2014a) have explored the $f(R)$ theory with exponential and power-law forms of bouncing cosmology. Shabani and Ziaie (2018) have worked on bouncing cosmological solutions from $f(R,T)$ gravity. Tripathy et al. (2019) have studied bouncing cosmology in an extended theory of gravity. Sahoo et al. (2020) have investigated the bouncing scenario in $f(R,T)$ gravity. Bamba et al. (2014b) have studied the bouncing cosmology in a modified Gauss–Bonnet gravity. Caruana et al. (2020) have studied the cosmological bouncing solutions in $f(T,B)$ gravity. Debnath and Paul (2021) have worked on the bouncing scenario with causal cosmology. Nojiri et al. (2016) have studied the bounce universe history from a unimodular $f(R)$ gravity.

This paper is organised as follows: In Section 2, the general formalism of $f(R,T)$ gravity and the field equations of $f(R,T)$ gravity are derived. Section 3 provides solutions to the field equations for three models, and Section 4 is mainly concerned with physical and geometrical properties. Finally, Section 5 contains conclusions.

2. GENERAL MATHEMATICAL FORMULATION OF $f(R,T)$ MODEL

$f(R,T)$ gravity is essential in providing a complete discussion on rapid expansion without the help of exotic matter. In 2010, Harko and Lobo developed the $f(R,L_m)$ theory, where R is the Ricci scalar and L_m stands for the matter Lagrangian density. The $f(R,T)$ gravity is a modified theory where the Lagrangian density is an arbitrary function $f(R,T)$ of the Ricci scalar R, and the trace of the energy-momentum tensor T. The T-dependence in $f(R,T)$ gravity may appear from the presence of imperfect fluids or quantum effects. The action integral for $f(R,T)$ gravity is as follows

$$S=\int\left[\frac{1}{16\pi}f(R,T)+L_m\right]\sqrt{-g}d^4x, \tag{1}$$

here, we take geometrical units $G=c=1$. Now, varying the above equation with respect to the fundamental tensor component g_{ij} yields the field equation

$$\left.\begin{aligned} f_R(R,T)R_{ij}-\frac{1}{2}f(R,T)g_{ij}+(g_{ij}\Box-\nabla_i\nabla_j)\\ f_R(R,T)=8\pi T_{ij}-f_T(R,T)\theta_{ij}-f_T(R,T)T_{ij}, \end{aligned}\right\} \tag{2}$$

here, ∇_i is the covariant derivative and $\Box=\nabla_i\nabla_j$ is the D'Alembert operator. $f_R(R,T)$ and $f_T(R,T)$ represent the derivatives of $f(R,T)$ with respect to R and T, respectively, and R_{ij} is the Ricci tensor. We have

$$\theta_{ij}=-2T_{ij}+g_{ij}L_m-2g^{lk}\frac{\partial^2 L_m}{\partial g^{ij}g^{lk}}. \tag{3}$$

The energy-momentum tensor T_{ij} is defined as

$$T_{ij}=\mathrm{diag}(\rho,-p,-p,-p), \tag{4}$$

where p and ρ are pressure and energy density of the fluid, respectively. Many researchers have investigated the energy-momentum tensor as a perfect fluid, mentioned in references (Ray 1982, Rao et al. 2008, Pradhan and Jotania 2011, Pradhan et al. 2007). Here, we consider $L_m=-p$ (Bertolami et al. 2007, Bisabr 2013, Sotiriou and Faraoni 2008) and θ_{ij} becomes

$$\theta_{ij}=-2T_{ij}-pg_{ij}, \tag{5}$$

and the trace of stress energy tensor is

$$T=\rho-3p. \tag{6}$$

By using the above equation, the $f(R,T)$ field Eq. (1) is obtained as

$$\left.\begin{aligned} G_{ij} = \frac{1}{f_R(R,T)}\Big[&[8\pi + f_T(R,T)]T_{ij} \\ &+ pf_T(R,T)g_{ij} + [\frac{1}{2}f(R,T) \\ &-\frac{1}{2}Rf_R(R,T)]g_{ij} \\ &-(g_{ij}\Box - \nabla_i\nabla_j)f_R(R,T)\Big], \end{aligned}\right\} \quad (7)$$

where G_{ij} is the Einstein tensor expressed as $R_{ij} - \frac{1}{2}Rg_{ij}$.

3. METRIC AND SOLUTIONS OF THE FIELD EQUATIONS

The spatially homogenous and anisotropic Bianchi-type cosmological models play a crucial role in the early universe. The investigation of anisotropic geometries is attaining more significance as a result of the recent Planck probe findings. The isotropy of CMBR and reflection of the amount of helium produced in the early stages of the universe's evolution fascinate in working on anisotropic cosmological models. Theoretical arguments and modern experimental evidence from the CMBR suggest the presence of an anisotropic phase which is later referred to as isotropic one. The authors who explored the anisotropic universe are given in (Vijaya Santhi et al. 2018, Reddy et al. 2016, Mishra et al. 2018, Sahoo et al. 2016, Vinutha et al. 2021a, Vinutha and Kavya 2022, Rao et al. 2015, Chaubey and Shukla 2013). Bianchi type models were examined because of less symmetric nature and they aid in finding more general cosmological models than the FRW model. The Bianchi-type III, V, VI_0 metric is given by

$$ds^2 = dt^2 - L^2dx^2 - M^2e^{-2x}dy^2 - N^2e^{-2kx}dz^2, \quad (8)$$

where L, M, and N are metric potentials, and functions of cosmic time t. Here, the co-moving coordinates are (t, x, y, z). k is an arbitrary constant, and here, we take $k = 0$ for Bianchi-III, $k = 1$ for Bianchi-V, and $k = -1$ for Bianchi-VI_0 metric, respectively.

3.1. Bianchi *III* cosmological model ($k = 0$)

The field equations Eq. (4) and Eq. (7) for metric Eq. (8) in the case $k = 0$ are given as follows, and these are the simplified equations after substitution $L = M$ which is the condition obtained from Bianchi - III metric field equations:

$$\left.\begin{aligned} &\frac{\ddot{L}}{L} + \frac{\ddot{N}}{N} + \frac{\dot{L}\dot{N}}{LN} = \\ &\frac{-(8\pi + \frac{3\lambda}{2})p}{1 - \nu\,\mathrm{sech}^2(\frac{R}{\gamma})} + \frac{\lambda\rho}{2(1 - \nu\,\mathrm{sech}^2(\frac{R}{\gamma}))} \\ &- \frac{\nu\gamma\tanh(\frac{R}{\gamma})}{2(1 - \nu\,\mathrm{sech}^2(\frac{R}{\gamma}))} + \frac{\nu R\,\mathrm{sech}^2(\frac{R}{\gamma})}{2(1 - \nu\,\mathrm{sech}^2(\frac{R}{\gamma}))} \\ &- \frac{2\nu\,\mathrm{sech}^2(\frac{R}{\gamma})\tanh(\frac{R}{\gamma})}{\gamma(1 - \nu\,\mathrm{sech}^2(\frac{R}{\gamma}))}\Big[\Big(\frac{\dot{L}}{L} + \frac{\dot{N}}{N}\Big)\dot{R} + \ddot{R}\Big] \\ &- \frac{2\dot{R}^2\nu\,\mathrm{sech}^2(1 - 3\tanh^2(\frac{R}{\gamma}))}{\gamma^2(1 - \nu\,\mathrm{sech}^2(\frac{R}{\gamma}))}. \end{aligned}\right\} \quad (9)$$

$$\left.\begin{aligned} &\frac{2\ddot{L}}{L} + \frac{\dot{L}^2}{L^2} - \frac{1}{L^2} = \\ &\frac{-(8\pi + \frac{3\lambda}{2})p}{1 - \nu\,\mathrm{sech}^2(\frac{R}{\gamma})} + \frac{\lambda\rho}{2(1 - \nu\,\mathrm{sech}^2(\frac{R}{\gamma}))} \\ &- \frac{\nu\gamma\tanh(\frac{R}{\gamma})}{2(1 - \nu\,\mathrm{sech}^2(\frac{R}{\gamma}))} + \frac{\nu R\,\mathrm{sech}^2(\frac{R}{\gamma})}{2(1 - \nu\,\mathrm{sech}^2(\frac{R}{\gamma}))} \\ &- \frac{2\nu\,\mathrm{sech}^2(\frac{R}{\gamma})\tanh(\frac{R}{\gamma})}{\gamma(1 - \nu\,\mathrm{sech}^2(\frac{R}{\gamma}))}\Big[\Big(\frac{2\dot{L}}{L}\Big)\dot{R} + \ddot{R}\Big] \\ &- \frac{2\dot{R}^2\nu\,\mathrm{sech}^2(1 - 3\tanh^2(\frac{R}{\gamma}))}{\gamma^2(1 - \nu\,\mathrm{sech}^2(\frac{R}{\gamma}))}. \end{aligned}\right\} \quad (10)$$

$$\left.\begin{aligned} \frac{\dot{L}^2}{L^2} + \frac{2\dot{L}\dot{N}}{LN} - \frac{1}{L^2} = &\frac{(8\pi + \frac{3\lambda}{2})\rho}{1 - \nu\,\mathrm{sech}^2(\frac{R}{\gamma})} \\ &- \frac{\lambda p}{2(1 - \nu\,\mathrm{sech}^2(\frac{R}{\gamma}))} \\ &- \frac{\nu\gamma\tanh(\frac{R}{\gamma})}{2(1 - \nu\,\mathrm{sech}^2(\frac{R}{\gamma}))} \\ &+ \frac{\nu R\,\mathrm{sech}^2(\frac{R}{\gamma})}{2(1 - \nu\,\mathrm{sech}^2(\frac{R}{\gamma}))} \\ - \frac{2\dot{R}\nu\,\mathrm{sech}^2(\frac{R}{\gamma})\tanh(\frac{R}{\gamma})}{\gamma(1 - \nu\,\mathrm{sech}^2(\frac{R}{\gamma}))}&\Big[\frac{2\dot{L}}{L} + \frac{\dot{N}}{N}\Big]. \end{aligned}\right\} \quad (11)$$

3.1.1. *Solutions of the field equations*

Two constraints are needed to procure the solutions of the above highly non-linear field equations Eq. (9)-Eq. (11), because it is evident from the field equations that the number of equations is less than the number of unknowns.

i) The first constraint is the relationship between the expansion scalar and shear scalar θ be proportional to σ. As a result of this constraint, the metric potentials L and N have the following relation

$$L = N^m, \tag{12}$$

where $m \neq 0, 1$ is a constant. The Thorne (1967) work can describe the physical reason for this supposition, i.e., the Hubble expansion of the universe is currently isotropic by approximately 30% according to the observations of the velocity redshift relation for extragalactic sources. More precisely, redshift studies place the limit $\frac{\sigma}{H} \leq 0.30$ on the ratio of shear (σ) to Hubble constant (H) in the neighbourhood of our Galaxy. (Kantowski and Sachs 1966, Kristian and Sachs 1966). Inspired by this, the first constraint is used in our work. In recent works, such as observational constraints on the expansion scalar, and shear relation in the locally rotationally symmetric Bianchi-I model (Singh et al. 2025), it can be observed that this relation has been probed for its observational compatibility with the data of different origins.

ii)The exponential scale factor for the bouncing scenario is considered as

$$a(t) = e^{\zeta t^2}, \tag{13}$$

where ζ is a positive constant. The main reason for exponential bouncing scale factors is to overcome the Big Bang singularity problem by replacing the infinitely dense point of origin with a smooth contracting-to-expanding phase. Cai et al. (2012) originally used this model to describe the non-singular bounce following an ekpyrotic contraction phase. The concept of a symmetric-bounce is based on the assumption that the universe goes through a contraction phase after expanding, reaching a minimum size (the bounce point), and then expanding again. The term symmetric in this regard relates to the behaviour of cosmic dynamics throughout contraction and expansion. This concept has importance in theoretical cosmology, the bouncing universe scenario, and other modified gravity theories. These theories try to address cosmological issues including the nature of the big bang singularity and the genesis of the universe. In general, the bouncing scenario divides the universe into two eras one is contraction and another is expansion. Here, the bounce happens at $t = 0$, before the bounce, the universe indicates contraction at $t < 0$, and after the bounce, the universe indicates expansion at $t > 0$.

The mean Hubble parameter for the Bianchi -III model is

$$H = \frac{1}{3}\Big(\frac{2\dot{L}}{L} + \frac{\dot{N}}{N}\Big). \tag{14}$$

From Eqs. (12)-(14), we get

$$L = M = (e^{\zeta t^2})^{\frac{3m}{2m+1}}, \tag{15}$$

$$N = (e^{\zeta t^2})^{\frac{3}{2m+1}}. \tag{16}$$

Using Eqs. (15) and (16), the Bianchi type-III metric is obtained as

$$\begin{aligned} ds^2 = dt^2 - (e^{\zeta t^2})^{\frac{6m}{2m+1}} dx^2 \\ -(e^{\zeta t^2})^{\frac{6m}{2m+1}} e^{-2x} dy^2 - (e^{\zeta t^2})^{\frac{6}{2m+1}} dz^2. \end{aligned} \tag{17}$$

3.2. Pressure and density in case of Bianchi-III model

By solving Eqs. (9)-(11) we get values of p and ρ for the Bianchi-III model as

$$\begin{aligned} p = \frac{1}{4}\Big(\frac{\chi+\eta-2\beta-\phi_5-\phi_6+2\phi_7+2\phi_8}{\phi_2-\phi_1} \\ -\frac{\chi+\eta+2\beta+4\phi_3-4\phi_4+7\phi_5+3\phi_6+2\phi_7+2\phi_8}{\phi_1+\phi_2}\Big), \end{aligned} \tag{18}$$

$$\begin{aligned} \rho = \\ \frac{1}{4}\Big(\frac{\chi+\eta+2\beta+4\phi_3-4\phi_4+7\phi_5+3\phi_6+2\phi_7+2\phi_8}{\phi_1+\phi_2} \\ +\frac{\chi+\eta-2\beta-\phi_5-\phi_6+2\phi_7+2\phi_8}{\phi_2-\phi_1}\Big), \end{aligned} \tag{19}$$

The values of χ, η, β, and $\phi_i (i = 1, 2.....8)$ are given in Appendix.

3.3. Bianchi V cosmological model ($k = 1$)

The field equations Eq. (4) with Eq. (7) for the metric Eq. (8) in the case of $k = 1$ are given as follows

$$\left.\begin{aligned} \frac{\ddot{M}}{M} + \frac{\ddot{N}}{N} + \frac{\dot{M}\dot{N}}{MN} - \frac{1}{L^2} = \frac{-(8\pi+\frac{3\lambda}{2})p}{1-\nu\,\mathrm{sech}^2(\frac{R}{\gamma})} \\ +\frac{\lambda\rho}{2(1-\nu\,\mathrm{sech}^2(\frac{R}{\gamma}))} \\ -\frac{\nu\gamma\tanh(\frac{R}{\gamma})}{2(1-\nu\,\mathrm{sech}^2(\frac{R}{\gamma}))} \\ +\frac{\nu R\,\mathrm{sech}^2(\frac{R}{\gamma})}{2(1-\nu\,\mathrm{sech}^2(\frac{R}{\gamma}))} \\ -\frac{2\nu\,\mathrm{sech}^2(\frac{R}{\gamma})\tanh(\frac{R}{\gamma})}{\gamma(1-\nu\,\mathrm{sech}^2(\frac{R}{\gamma}))}\Big[\Big(\frac{\dot{M}}{M}+\frac{\dot{N}}{N}\Big)\dot{R}+\ddot{R}\Big] \\ -\frac{2\dot{R}^2\nu\,\mathrm{sech}^2(1-3\tanh^2(\frac{R}{\gamma}))}{\gamma^2(1-\nu\,\mathrm{sech}^2(\frac{R}{\gamma}))}. \end{aligned}\right\} \tag{20}$$

$$\left.\begin{aligned}\frac{\ddot{L}}{L}+\frac{\ddot{N}}{N}+\frac{\dot{L}\dot{N}}{LN}-\frac{1}{L^2}&=\frac{-(8\pi+\frac{3\lambda}{2})p}{1-\nu\,\mathrm{sech}^2(\frac{R}{\gamma})}\\ +\frac{\lambda\rho}{2(1-\nu\,\mathrm{sech}^2(\frac{R}{\gamma}))}&-\frac{\nu\gamma\tanh(\frac{R}{\gamma})}{2(1-\nu\,\mathrm{sech}^2(\frac{R}{\gamma}))}\\ &+\frac{\nu R\,\mathrm{sech}^2(\frac{R}{\gamma})}{2(1-\nu\,\mathrm{sech}^2(\frac{R}{\gamma}))}\\ -\frac{2\nu\,\mathrm{sech}^2(\frac{R}{\gamma})\tanh(\frac{R}{\gamma})}{\gamma(1-\nu\,\mathrm{sech}^2(\frac{R}{\gamma}))}&\Big[\Big(\frac{\dot{L}}{L}+\frac{\dot{N}}{N}\Big)\dot{R}+\ddot{R}\Big]\\ -\frac{2\dot{R}^2\nu\,\mathrm{sech}^2(1-3\tanh^2(\frac{R}{\gamma}))}{\gamma^2(1-\nu\,\mathrm{sech}^2(\frac{R}{\gamma}))}&.\end{aligned}\right\}\quad(21)$$

$$\left.\begin{aligned}\frac{\ddot{L}}{L}+\frac{\ddot{M}}{M}+\frac{\dot{L}\dot{M}}{LM}-\frac{1}{L^2}&=\frac{-(8\pi+\frac{3\lambda}{2})p}{1-\nu\,\mathrm{sech}^2(\frac{R}{\gamma})}\\ +\frac{\lambda\rho}{2(1-\nu\,\mathrm{sech}^2(\frac{R}{\gamma}))}&-\frac{\nu\gamma\tanh(\frac{R}{\gamma})}{2(1-\nu\,\mathrm{sech}^2(\frac{R}{\gamma}))}\\ &+\frac{\nu R\,\mathrm{sech}^2(\frac{R}{\gamma})}{2(1-\nu\,\mathrm{sech}^2(\frac{R}{\gamma}))}\\ -\frac{2\nu\,\mathrm{sech}^2(\frac{R}{\gamma})\tanh(\frac{R}{\gamma})}{\gamma(1-\nu\,\mathrm{sech}^2(\frac{R}{\gamma}))}&\Big[\Big(\frac{\dot{L}}{L}+\frac{\dot{M}}{M}\Big)\dot{R}+\ddot{R}\Big]\\ -\frac{2\dot{R}^2\nu\,\mathrm{sech}^2(1-3\tanh^2(\frac{R}{\gamma}))}{\gamma^2(1-\nu\,\mathrm{sech}^2(\frac{R}{\gamma}))}&.\end{aligned}\right\}\quad(22)$$

$$\left.\begin{aligned}\frac{\dot{L}\dot{M}}{LM}+\frac{\dot{M}\dot{N}}{MN}+\frac{\dot{L}\dot{N}}{LN}-\frac{3}{L^2}&=\frac{(8\pi+\frac{3\lambda}{2})\rho}{1-\nu\,\mathrm{sech}^2(\frac{R}{\gamma})}\\ -\frac{\lambda p}{2(1-\nu\,\mathrm{sech}^2(\frac{R}{\gamma}))}&-\frac{\nu\gamma\tanh(\frac{R}{\gamma})}{2(1-\nu\,\mathrm{sech}^2(\frac{R}{\gamma}))}\\ &+\frac{\nu R\,\mathrm{sech}^2(\frac{R}{\gamma})}{2(1-\nu\,\mathrm{sech}^2(\frac{R}{\gamma}))}\\ -\frac{2\dot{R}\nu\,\mathrm{sech}^2(\frac{R}{\gamma})\tanh(\frac{R}{\gamma})}{\gamma(1-\nu\,\mathrm{sech}^2(\frac{R}{\gamma}))}&\Big[\frac{\dot{L}}{L}+\frac{\dot{M}}{M}+\frac{\dot{N}}{N}\Big].\end{aligned}\right\}\quad(23)$$

$$\frac{1}{L^2}\Big[\frac{\dot{M}}{M}+\frac{\dot{N}}{N}-\frac{2\dot{L}}{L}\Big]=0.\quad(24)$$

3.3.1. *Solutions of the field equations*

Two constraints are needed to procure the solutions of the above highly non-linear field equations Eqs. (20)-(23), because, from the field equations, it is evident that the number of equations is less than the number of unknowns.

i) The first constraint is the relationship between expansion scalar and shear scalar (θ is proportional to σ). As a result of this constraint, the metric potentials (M and N) are connected by the relation

$$M=N^m,\quad(25)$$

$m\neq 0,1$ is constant.

ii) The exponential scale factor for bouncing scenario is assumed as shown above in Eq. (13). The mean Hubble parameter for Bianchi -V model is

$$H=\frac{1}{3}\Big(\frac{\dot{L}}{L}+\frac{\dot{M}}{M}+\frac{\dot{N}}{N}\Big).\quad(26)$$

From Eqs. (25), (13) and (26), we get

$$L=e^{\zeta t^2},\quad(27)$$

$$M=(e^{\zeta t^2})^{\frac{2m}{m+1}},\quad(28)$$

$$N=(e^{\zeta t^2})^{\frac{2}{m+1}}.\quad(29)$$

Using Eqs. (27)-(29), the Bianchi type-V metric is obtained as

$$\begin{aligned}ds^2=dt^2-(e^{\zeta t^2})^2dx^2-(e^{\zeta t^2})^{\frac{4m}{2m+1}}e^{-2x}dy^2\\ -(e^{\zeta t^2})^{\frac{4}{2m+1}}e^{-2x}dz^2.\end{aligned}\quad(30)$$

3.3.2. *Pressure and density in the case of Bianchi-V model*

By solving Eqs. (20)-(23) we get the values of p and ρ for the Bianchi-V model as

$$\begin{aligned}p=\frac{1}{6}\Big(&\frac{\chi_1+\eta_1+\beta_1-3\epsilon-\iota_5-\iota_6+3\iota_7+3\iota_8-\iota_9}{\iota_2-\iota_1}\\ &-\frac{\chi_1+\eta_1+\beta_1+3\epsilon+6\iota_3-6\iota_4}{\iota_1+\iota_2}\\ &-\frac{5\iota_5+5\iota_6+3\iota_7+3\iota_8+5\iota_9}{\iota_1+\iota_2}\Big),\end{aligned}\quad(31)$$

$$\begin{aligned}\rho=\frac{1}{6}\Big(&\frac{\chi_1+\eta_1+\beta_1+3\epsilon+6\iota_3-6\iota_4}{\iota_1+\iota_2}\\ &+\frac{5\iota_5+5\iota_6+3\iota_7+3\iota_8+5\iota_9}{\iota_1+\iota_2}\\ &+\frac{\chi_1+\eta_1+\beta_1-3\epsilon-\iota_5-\iota_6+3\iota_7+3\iota_8-\iota_9}{\iota_2-\iota_1}\Big),\end{aligned}\quad(32)$$

The values of χ_1, η_1, β_1, ϵ, and $\iota_i(i=1,2.....9)$ are given in Appendix.

3.4. Bianchi VI_0 cosmological model ($k=-1$)

The field equations Eq. (4) and Eq. (7) for the metric Eq. (8) in the case of $k=-1$ are given as follows, and these are the simplified equations after substitution $M=N$ which is the condition obtained from Bianchi - VI_0 metric field equations

$$\left.\begin{aligned}\frac{2\ddot{N}}{N}+\frac{\dot{N}^2}{N^2}+\frac{1}{L^2}&=\frac{-(8\pi+\frac{3\lambda}{2})p}{1-\nu\,\mathrm{sech}^2(\frac{R}{\gamma})}\\&+\frac{\lambda\rho}{2(1-\nu\,\mathrm{sech}^2(\frac{R}{\gamma}))}-\frac{\nu\gamma\tanh(\frac{R}{\gamma})}{2(1-\nu\,\mathrm{sech}^2(\frac{R}{\gamma}))}\\&+\frac{\nu R\,\mathrm{sech}^2(\frac{R}{\gamma})}{2(1-\nu\,\mathrm{sech}^2(\frac{R}{\gamma}))}\\&-\frac{2\nu\,\mathrm{sech}^2(\frac{R}{\gamma})\tanh(\frac{R}{\gamma})}{\gamma(1-\nu\,\mathrm{sech}^2(\frac{R}{\gamma}))}\Big[\Big(\frac{2\dot{N}}{N}\Big)\dot{R}+\ddot{R}\Big]\\&-\frac{2\dot{R}^2\nu\,\mathrm{sech}^2(1-3\tanh^2(\frac{R}{\gamma}))}{\gamma^2(1-\nu\,\mathrm{sech}^2(\frac{R}{\gamma}))}.\end{aligned}\right\}\quad(33)$$

$$\left.\begin{aligned}\frac{\ddot{L}}{L}+\frac{\ddot{N}}{N}+\frac{\dot{L}\dot{N}}{LN}-\frac{1}{L^2}&=\frac{-(8\pi+\frac{3\lambda}{2})p}{1-\nu\,\mathrm{sech}^2(\frac{R}{\gamma})}\\&+\frac{\lambda\rho}{2(1-\nu\,\mathrm{sech}^2(\frac{R}{\gamma}))}-\frac{\nu\gamma\tanh(\frac{R}{\gamma})}{2(1-\nu\,\mathrm{sech}^2(\frac{R}{\gamma}))}\\&+\frac{\nu R\,\mathrm{sech}^2(\frac{R}{\gamma})}{2(1-\nu\,\mathrm{sech}^2(\frac{R}{\gamma}))}\\&-\frac{2\nu\,\mathrm{sech}^2(\frac{R}{\gamma})\tanh(\frac{R}{\gamma})}{\gamma(1-\nu\,\mathrm{sech}^2(\frac{R}{\gamma}))}\Big[\Big(\frac{\dot{L}}{L}+\frac{\dot{N}}{N}\Big)\dot{R}+\ddot{R}\Big]\\&-\frac{2\dot{R}^2\nu\,\mathrm{sech}^2(1-3\tanh^2(\frac{R}{\gamma}))}{\gamma^2(1-\nu\,\mathrm{sech}^2(\frac{R}{\gamma}))}.\end{aligned}\right\}\quad(34)$$

$$\left.\begin{aligned}\frac{\dot{N}^2}{N^2}+\frac{2\dot{L}\dot{N}}{LN}-\frac{1}{L^2}&=\frac{(8\pi+\frac{3\lambda}{2})\rho}{1-\nu\,\mathrm{sech}^2(\frac{R}{\gamma})}\\&-\frac{\lambda p}{2(1-\nu\,\mathrm{sech}^2(\frac{R}{\gamma}))}-\frac{\nu\gamma\tanh(\frac{R}{\gamma})}{2(1-\nu\,\mathrm{sech}^2(\frac{R}{\gamma}))}\\&+\frac{\nu R\,\mathrm{sech}^2(\frac{R}{\gamma})}{2(1-\nu\,\mathrm{sech}^2(\frac{R}{\gamma}))}\\&-\frac{2\dot{R}\nu\,\mathrm{sech}^2(\frac{R}{\gamma})\tanh(\frac{R}{\gamma})}{\gamma(1-\nu\,\mathrm{sech}^2(\frac{R}{\gamma}))}\Big[\frac{\dot{L}}{L}+\frac{2\dot{N}}{N}\Big].\end{aligned}\right\}\quad(35)$$

3.4.1. *Solutions of the field equations*

Two constraints are needed to procure the solutions of the above highly non-linear field equations Eqs. (33)-(35), because, from the field equations, it is evident that the number of equations is less than the number of unknowns.

i) The first constraint is the relationship between expansion scalar and shear scalar (θ is proportional to σ). As a result of this constraint, the metric potentials (N and L) are connected by the relation

$$N=L^m, \tag{36}$$

here $m\neq 0,1$ is constant.

ii) The exponential scale factor for bouncing scenario is assumed as shown above in equation Eq. (13).

The mean Hubble parameter for the Bianchi -VI_0 model is

$$H=\frac{1}{3}\Big(\frac{\dot{L}}{L}+\frac{2\dot{N}}{N}\Big). \tag{37}$$

From equations Eqs. (36),(13) and (37), we get

$$L=(e^{\zeta t^2})^{\frac{3}{2m+1}}, \tag{38}$$

$$M=N=(e^{\zeta t^2})^{\frac{3m}{2m+1}}. \tag{39}$$

Using equations Eqs. (38)-(39), the Bianchi type-VI_0 is obtained as:

$$\begin{aligned}ds^2=dt^2-(e^{\zeta t^2})^{\frac{6}{2m+1}}dx^2-(e^{\zeta t^2})^{\frac{6m}{2m+1}}e^{-2x}dy^2\\-(e^{\zeta t^2})^{\frac{6m}{2m+1}}e^{2x}dz^2.\end{aligned} \tag{40}$$

3.4.2. *Pressure and density for the Bianchi-VI_0 model*

By solving Eqs. (33)-(35) we get the values of p and ρ for the Bianchi-VI_0 model as:

$$\begin{aligned}p=\frac{1}{4}\Big(&\frac{\chi_2+\eta_2-2\beta_2-\alpha_5+2\alpha_6+2\alpha_7-\alpha_8}{\alpha_2-\alpha_1}\\-&\frac{\chi_2+\eta_2+2\beta_2+4\alpha_3-4\alpha_4+7\alpha_5+2\alpha_6+2\alpha_7+3\alpha_8}{\alpha_1+\alpha_2}\Big),\end{aligned} \tag{41}$$

$$\begin{aligned}\rho=\frac{1}{4}\Big(&\frac{\chi_2+\eta_2+2\beta_2+4\alpha_3-4\alpha_4}{\alpha_1+\alpha_2}\\&+\frac{7\alpha_5+2\alpha_6+2\alpha_7+3\alpha_8}{\alpha_1+\alpha_2}\\&+\frac{\chi_2+\eta_2-2\beta_2-\alpha_5+2\alpha_6+2\alpha_7-\alpha_8}{\alpha_2-\alpha_1}\Big),\end{aligned} \tag{42}$$

The values of χ_2, η_2, β_2, and $\alpha_i (i=1,2.....8)$ are given in Appendix.

4. PROPERTIES OF THE MODELS:

All the physical and geometrical parameters of the obtained model are discussed thoroughly with the help of their plots with respect to time (t). The negative region of t, i.e., $t\leq 0$, indicates the contraction phase, whereas

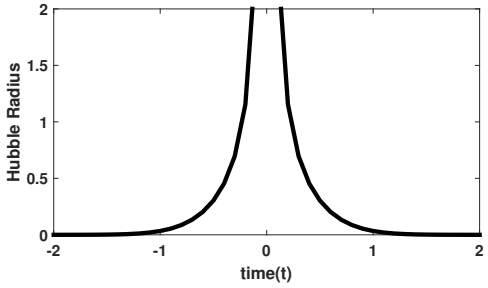

Fig. 1: Plot of the Hubble radius versus time (t).

the positive region of t, i.e., $t \geq 0$, indicates the expansion phase, and the bounce occurs at time zero, i.e. $t = 0$.

i) The Hubble sphere is defined by the Hubble radius and, at any cosmic time, the Hubble radius is the radial coordinate of the Hubble sphere boundary which is a closed 2-dimensional spatial surface. The Hubble sphere center is at the place of the observer and it is independent of the previous history or future of the cosmos. The Hubble radius parameter is described as:

$$R_H = \frac{1}{a(t)H(t)} = \frac{1}{e^{\zeta t^2} 2\zeta t}, \tag{43}$$

where $a(t)$ and $H(t)$ are the scale factor and Hubble parameter, respectively. From Fig. 1, it is observed that before the bounce, the Hubble radius increases with time, it blows up at $t = 0$, and after the bounce, the Hubble radius decreases with cosmic time.

ii) The spatial volume of the model is

$$V = a^3 = (e^{\zeta t^2})^3. \tag{44}$$

Fig. 2 shows the the volume decreases with time before the bounce at $t = 0$. After the bounce, the volume increases with time.

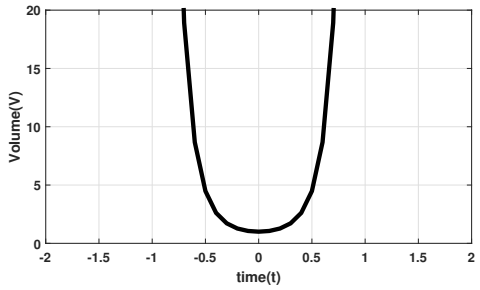

Fig. 2: Plot of volume (V) versus time (t).

iii) The expansion scalar θ is

$$\theta = u^i_{;i} = 3H = 6\zeta t. \tag{45}$$

iv) The shear scalar for Bianchi-III and Bianchi-VI_0 models is given by

$$\sigma^2 = \frac{3\zeta^2 t^2 (m-1)^2}{(m+1)^2}, \tag{46}$$

and the shear scalar for the Bianchi- V model is

$$\sigma^2 = \frac{4\zeta^2 t^2 (m-1)^2}{(m+1)^2}. \tag{47}$$

v) The mean anisotropy parameter A_h is defined based on the directional Hubble parameter, and mean Hubble parameter as

$$A_h = \frac{1}{3}\Big[\sum \Big(\frac{H_i - H}{H}\Big)^2\Big], \tag{48}$$

where $H_i, i = 1, 2, 3$, indicates the directional Hubble parameters for the coordinates of x, y, and z, respectively. The mean anisotropy parameter A_h for the Bianchi-III and Bianchi-VI_0 models is obtained as

$$A_h = \frac{2(m-1)^2}{(2m+1)^2}; m \neq 1, \tag{49}$$

and the mean anisotropy parameter A_h for the Bianchi-V model is obtained as

$$A_h = \frac{2(m-1)^2}{3(m+1)^2}; m \neq 1. \tag{50}$$

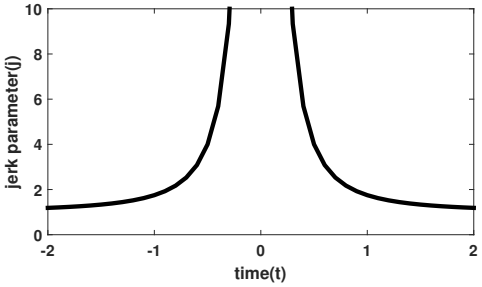

Fig. 3: Plot of jerk parameter (j) versus time (t).

4.1. Jerk parameter

The parameters such as the Hubble parameter, deceleration parameter, and jerk parameter are described by the first, second, and third derivatives of scale factor with respect to time t, respectively, and it is one of the most significant quantities for studying the universe evolution. The jerk parameter can be used to find departures from concordance with ΛCDM. It is unique characteristic for revealing hidden transitions between stages of various cosmic acceleration.

The jerk parameter is defined as

$$j = \frac{1}{aH^3}\frac{d^3a}{dt^3}. \tag{51}$$

For this model, the jerk parameter is

$$j = 1 + \frac{3}{2\zeta t^2}. \tag{52}$$

The value $j = 1$ is in the case of a flat ΛCDM model. The jerk parameter is positive for both the contracting and expanding universe, as shown in Fig. 3.

4.2. Deceleration parameter

One of geometrical parameters is the dimensionless deceleration parameter q, defined as

$$q = -1 + \frac{d}{dt}(\frac{1}{H}), \tag{53}$$

that can be used to determine the dynamics of the cosmos. Based on the sign of q (i.e., positive/negative), it can be observed whether the universe is accelerating/decelerating. The universe indicates a decelerating expansion when $q > 0$, expansion with constant rate when $q = 0$, accelerating power-law expansion when $-1 < q < 0$, exponential expansion when $q = -1$, and super-exponential expansion when $q < -1$. From Fig. 4, it is observed that $q < 0$ indicates a contracting and accelerating, whereas $q > 0$ shows an expanding and decelerating scenario.

For this model, the deceleration parameter is

$$q = -1 - \frac{1}{2\zeta t^2}. \tag{54}$$

The value of the deceleration parameter matches the observational values of SNe Ia, which represents an expanding universe (Clocchiatti et al. 2006, Riess et al. 2004, Tonry et al. 2003).

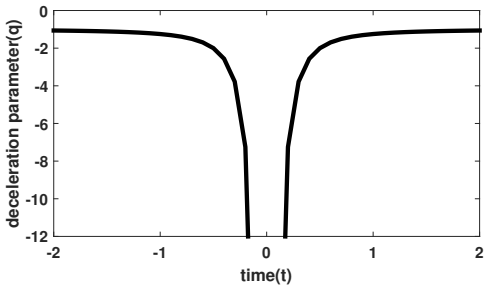

Fig. 4: Plot of deceleration parameter (q) versus time (t).

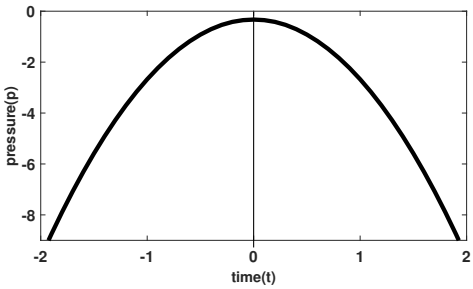

Fig. 5: Plot of pressure (p) versus time (t) for Bianchi-III model.

4.3. Pressure

Figs. 5, 6 and 7 show the sketch of pressure against time for the three models. In pressure graphs, it is observed that the pressure is in maximum at $t = 0$. Pressure is negative throughout space-time, it takes negative values all over the range, and negative pressure shows a rapid expansion.

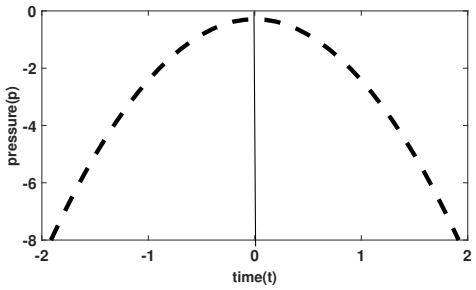

Fig. 6: Pressure (p) for Bianchi-V model.

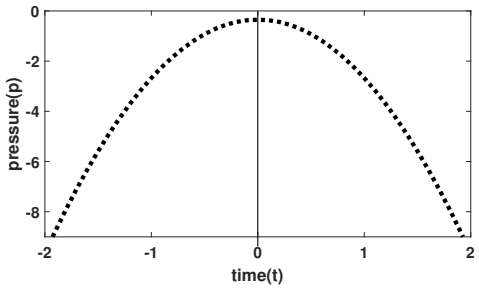

Fig. 7: Pressure (p) for Bianchi-VI_0 model.

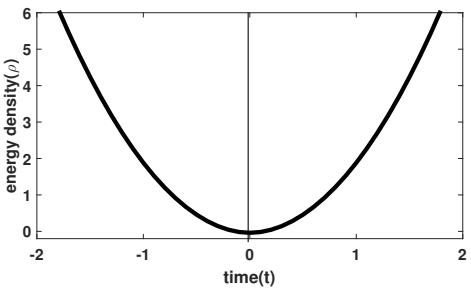

Fig. 8: Energy density (ρ) for Bianchi-III model.

4.4. Energy density

Figs. 8, 9 and 10 depict the evolution of the energy density of the three models. It is clear that the energy density is positive, and the curve is convex at the bounce. The energy density is positive throughout space-time, it takes positive values all over the range. In both, the pressure and energy density graphs, before the bounce and after the bounce the curves, are symmetric.

4.5. EoS parameter

The term EoS parameter is defined as the ratio of pressure and energy density i.e., $\omega = \frac{p}{\rho}$, and is widely used to categorize many regions of the expanding cosmos. It distinguishes between the decelerated and accel-

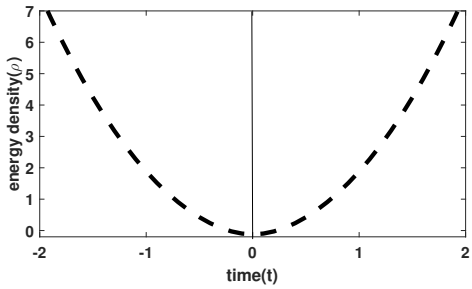

Fig. 9: Energy density (ρ) for Bianchi-V model.

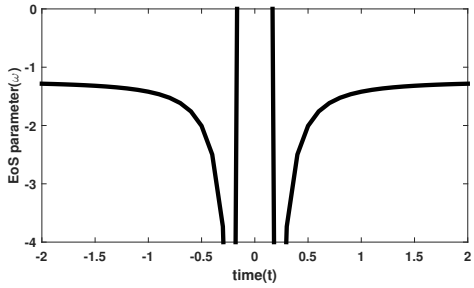

Fig. 11: EoS parameter (ω) for Bianchi-III model.

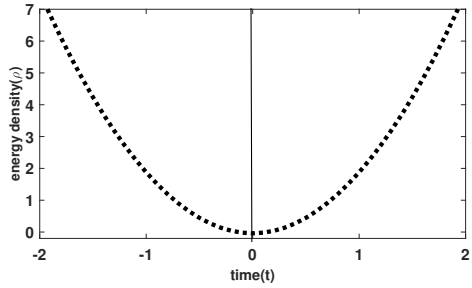

Fig. 10: Energy density (ρ) for Bianchi-VI_0 model.

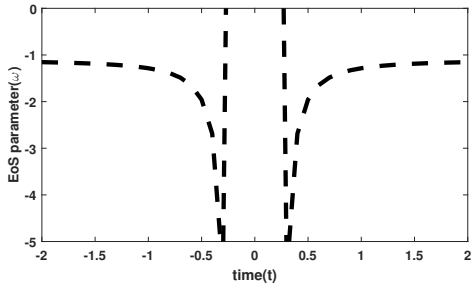

Fig. 12: EoS parameter (ω) for Bianchi-V model.

erated stages of the expanding universe in the era listed below. In the quintessence region, the EoS parameter lies within the range of $-1 < \omega < -\frac{1}{3}$, in the phantom phase, the EoS parameter is in the range of less than -1 (i.e., $\omega < -1$), and in the quintom, $\omega = -1$. For a stiff fluid-dominated universe, dust fluid, radiation, and vacuum; the values of the EoS parameter are $\omega = (1, 0, \frac{-1}{3}, -1)$. However, the EoS parameter should not be considered constant as it varies with time (t), or redshift (z). Figs. 11, 12 and 13 of the EoS parameter are drawn against time and, from the figures, it can be noticed that it decreases with time before the bounce, that is in the phantom region ($\omega < -1$), at $t = 0$ we have some vertical lines, and, after the bounce, the EoS parameter increases with time. It is clear that ω evolved from $\omega > -1$ to $\omega < -1$, symbolizing several phases of the cosmos, such as quintessence ($\omega > -1$) and phantom ($\omega < -1$). Using SNe Ia data from various surveys, the Pantheon study produced the result $\omega = -1.026 \pm 0.041$ (Scolnic et al. 2018), which is for a flat CDM model, and, after merging with the CMB constraints, it results in $\omega = -0.978 \pm 0.059$. Observational constraints from the Planck Collaboration (Planck Collaboration et al. 2014) and WMAP (Hinshaw et al. 2013) place the EoS parameter in the ranges (i) $-0.92 \leq \omega \leq -1.26$ (Planck + WP + Union 2.1), (ii) $-0.89 \leq \omega \leq -1.38$ (Planck + WP + BAO), and (iii) $-0.983 \leq \omega \leq -1.162$ (WMAP + eCMB + BAO + H0). The three models match the above observational data, which is a good result.

4.6. Energy conditions

Energy conditions are attractive because of the casual and geodesic structure of space-time, along with the attractive nature of gravity, and it is used to study the behavior of cosmological solutions throughout the cosmos. Also, energy conditions are well understood for implementing the positiveness of the stress-energy tensor in the presence of matter. The energy conditions originate from the Ray-chaudhuri equations, which allow us to study the complete spacetime structure without having to solve Einstein's equations precisely. These conditions are the linear combination of pressure and energy density, and from these conditions, we perceive that the pressure and energy density cannot be negative. Most commonly used inequalities of energy conditions in terms of a perfect fluid matter and stress-energy tensor T are

- NEC states that $T_{ij}u^i u^j \geq 0$ for any null vector u^i, and it is acquired as $\rho + p \geq 0$.
- WEC states that $T_{ij}u^i u^j \geq 0$, for any timelike vector and one can obtain $\rho \geq 0$, $\rho + p \geq 0$.
- DEC given by $T^{ij}u_j$ is a non-spacelike vector, where u^i is a timelike vector, thus $u^i u_i = -1$, $\rho \geq 0$, following that $\rho \pm p \geq 0$.
- SEC written as $(T_{ij} - \frac{1}{2}Tg_{ij})u^i u^j \geq 0$, for all timelike vector u^i, which leads to $\rho + 3p \geq 0$, $\rho + p \geq 0$.

The attractive essence of gravity is described by NEC, while SEC is beneficial for studying the Hawking Penrose singularity theorem. DEC is used to prove the positive mass theory, and energy transfer velocity cannot exceed the speed of light. For WEC, the requirement necessitates that the energy density measured by every observer must always be positive, and for the DEC energy density measured by any observer is non-negative. Energy conditions have been investigated in various modified theories

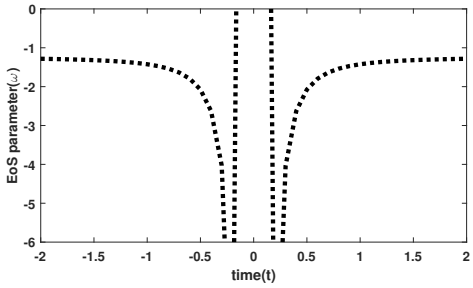

Fig. 13: EoS parameter (ω) for Bianchi-VI_0 model.

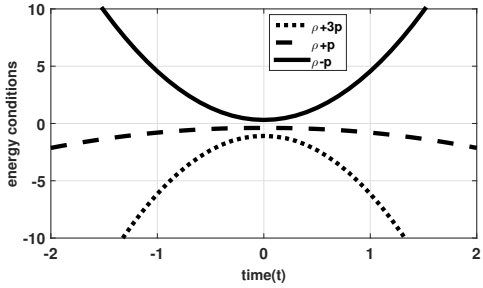

Fig. 16: Energy conditions for Bianchi-VI_0 model.

such as $f(R)$ (Santos et al. 2007, Wang et al. 2010, Bertolami and Sequeira 2009), $f(T)$ (Jamil et al. 2013, Liu and Reboucas 2012), $f(R, L_m)$ (Wang and Liao 2012), and $f(R, T)$ (Sharif and Zubair 2013, Capozziello et al. 2014, 2015). The behavior of energy conditions are discussed in detail with the help of their plots. As observed from Figs. 14, 15 and 16, DEC is fulfilled, that is $\rho - p \geq 0$, whereas SEC and NEC are violated, $\rho + 3p \leq 0$ and $\rho + p \leq 0$ for three models.

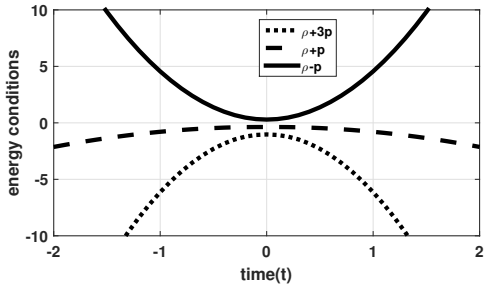

Fig. 14: Energy conditions for Bianchi-III model.

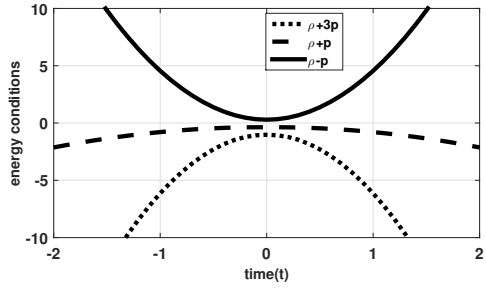

Fig. 15: Energy conditions for Bianchi-V model.

4.7. Stability analysis

The perturbation technique (Yadav et al. 2019, Chen and Kao 2001, Saha et al. 2012) is basically used for finding approximate solutions to the obtained exact solutions. The stability of the solution against metric perturbation will be studied in this section.

$$a_i \to a_{Bi} + \delta a_i = a_{Bi}(1 + \delta b_i). \tag{55}$$

The perturbation of volume scale factor, directional Hubble factors, and mean Hubble factor are given as

$$\left.\begin{aligned} V &\to V_B + V_B \sum_i \delta b_i, \\ \theta_i &\to \theta_{Bi} + \sum_i \delta b_i, \\ \theta &\to \theta_B + \frac{1}{3}\sum_i \delta b_i. \end{aligned}\right\} \tag{56}$$

The metric perturbations δbi are shown in the equations given below.

$$\sum_i \delta\ddot{b}_i + 2\sum_i \theta_{Bi}\delta\dot{b}_i = 0, \tag{57}$$

$$\delta\ddot{b}_i + \frac{\dot{V}_B}{V_B}\delta\dot{b}_i + \sum_j \delta\dot{b}_j\theta_{Bi} = 0, \tag{58}$$

$$\sum_i \delta\dot{b}_i = 0. \tag{59}$$

From equations Eqs. (57) - (59), we get

$$\delta\ddot{b}_i + \frac{\dot{V}_B}{V_B}\delta\dot{b}_i = 0, \tag{60}$$

where V_B is the background spatial volume and, in our case, V_B is

$$V_B = e^{3\zeta t^2}. \tag{61}$$

Using the above equations, we get

$$\delta b_i = c_1 + c\Big(\frac{\sqrt{\pi}}{2\sqrt{3\zeta}} erf(\sqrt{3\zeta}t)\Big), \tag{62}$$

where c_1 and c are constants of integration.

Hence, the actual fluctuations $\delta a_i = a_{Bi}\delta b_i$ is

$$\delta a_i = c_1 e^{-3\zeta t^2} + ce^{-3\zeta t^2}\Big(\frac{\sqrt{\pi}}{2\sqrt{3\zeta}} erf(\sqrt{3\zeta}t)\Big). \tag{63}$$

From Fig. 17 it is clear that δa_i begins with small positive value and approaches zero i.e. $\delta a_i \to 0$ as $t \to \infty$. Hence, the background solution is stable against perturbation of gravitational field.

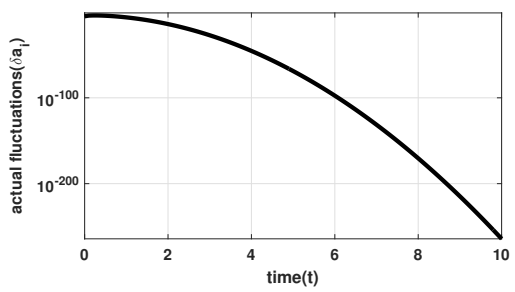

Fig. 17: Actual fluctuations (δa_i) versus time (t).

5. CONCLUSIONS

For cosmologists studying the dynamics of the cosmos has become a significant aspect of their work. The present research study focuses on the Bianchi-III, V, and VI_0 bouncing cosmological models in $f(R,T)$ gravity. A cosmological model is a mathematical representation of the universe that elucidates the geometry of space and time as well as the distribution and nature of matter. Current cosmological interests encourage us to study modified theories of gravity that aim to explain the cosmic speed-up. The bouncing scale factor is used to solve the field equations and provide precise solutions. Here, we examined the non-singular bouncing scale factor, and the importance of the non-singular bouncing cosmology is that it avoids the singularity problem. According to the current interpretation of the bouncing cosmology, the universe's expansion is preceded by a period of contraction, after which a non-vanishing bouncing point connects the contraction and expansion. All graphs are drawn with respect to time (t) and discuss the behavior of all parameters of the three models. The following conclusions were obtained after observing the parameters:

- From Fig. 1, as cosmic time moves away from bounce, the Hubble radius reduces to smaller values, i.e., it reaches zero, and near the bounce, the Hubble radius represents a narrow region. As observed from Fig. 2, it is noticed that the volume has a minimum value at $t = 0$, decreases with time before the bounce, and increases with time after the bounce.
- Models that include a cosmic jerk better depict transitions between stages of distinct cosmic accelerations. The jerk parameter is plotted against time (t) in Fig. 3. Due to the vanishing nature of the Hubble rate at bounce, the jerk parameter has a singular value at the bouncing epoch. From Fig. 3, it is clear that, the jerk parameter reaches ΛCDM as $t \to \infty$ and $t \to -\infty$.
- The graph of deceleration parameter is drawn with respect to time (t). From Fig. 4, it is obvious that the deceleration parameter is negative in both phases. The observations of distant type Ia supernovae show that q is negative, implying the universe's expansion is speeding up.
- The pressure is negative, and the energy density is positive in all three models, as seen in Figs. 5 to 7, and 8 to 10. The rapid expansion of the cosmos is attributed to the negative pressure and positive energy density.
- The figures showing the EoS parameter indicate its dependence on cosmic time in the three models. The model starts from the quintessence era with vertical lines and reaches the phantom region. Furthermore, these models exhibit a quintom model, as evidenced by observational data (Zhao et al. 2007, Feng et al. 2005).
- From Figs. 14 to 16, it is observed that the energy conditions are drawn with respect to time. NEC and SEC are violated in the three models, whereas DEC is fulfilled. Since NEC is violated, the models evolve in the phantom phase in both phases of the bouncing universe of the EoS parameter. The violation of SEC corroborates with rapid expansion, and all parameters discovered here represent the aspects of the universe's current phase.
- The stability analysis of the background solutions of the obtained models is verified using perturbation techniques, and it is clear that the background solutions are stable against the perturbation of the gravitational field, as shown in Fig. 17. It is observed that for all the three models, the graphs of pressure and energy density show a negative pressure and positive energy density, which may be responsible for accelerated expansion of the universe. However, in plots of the EoS parameter, small variations are seen. Among the three models, Bianchi-V is more stable, symmetric near $X = 0$, and satisfies the observational data more accurately. The remaining two models are consistent with the observational data more accurately. From the plots of energy conditions of the three anisotropic models, it is observed that all of them satisfy DEC ensuring physical acceptability of the matter distribution. However, SEC and NEC are violated in all models. The extent of violation is the highest in the Bianchi-V model, where the values of SEC and NEC show the largest negative departure. The Bianchi VI_0 model exhibits a moderate extent of violation with a slightly negative value. In contrast, the Bianchi III model shows the least departure from SEC and NEC making it comparatively more stable and physically viable among the three. In summary, while all models align with observational data and depict a late-time acceleration, the hierarchy of stability and energy-condition compliance suggests that the three models provide an anisotropic framework that is physically consistent.

  The models presented in this study are capable of describing the universe's evolution accuratly and producing desirable outcomes which support the present observational data. Finally, despite the absence of any exotic fluid, the present universe is found to

undergo accelerated expansion, representing a significant result of this study. This work could be extended to other anisotropic models in the future, and similarities and differences among them could be investigated.

Acknowledgements – The author Vinutha Tummala would like to thank the authorities of the IUCAA, Pune, India for providing the facilities under visiting associateship programme. Authors are very much thankful to the anonymous reviewer and editor for the valuable suggestions and constructive comments which have significantly improved the paper in terms of research quality and presentation.

REFERENCES

Amendola, L. and Tsujikawa, S. 2010, Dark Energy: Theory and Observations (Cambridge University Press)
Appleby, S. and Battye, R. 2007, PhLB, 654, 7
Bamba, K., Makarenko, A. N., Myagky, A. N., Nojiri, S. and Odintsov, S. D. 2014a, JCAP, 2014, 008
Bamba, K., Makarenko, A. N., Myagky, A. N. and Odintsov, S. D. 2014b, PhLB, 732, 349
Banerjee, A., Sakallı, İ., Dayanandan, B. and Pradhan, A. 2025, Chinese Physics C, 49, 015102
Bertolami, O. and Sequeira, M. C. 2009, PhRvD, 79, 104010
Bertolami, O., Böhmer, C. G., Harko, T. and Lobo, F. S. N. 2007, PhRvD, 75, 104016
Bisabr, Y. 2013, GReGr, 45, 1559
Cai, Y.-F., Easson, D. A. and Brandenberger, R. 2012, JCAP, 08, 020
Caldwell, R. R. 2002, PhLB, 545, 23
Capozziello, S., Lobo, F. S. N. and Mimoso, J. P. 2014, PhLB, 730, 280
Capozziello, S., Lobo, F. S. N. and Mimoso, J. P. 2015, PhRvD, 91, 124019
Caruana, M., Farrugia, G. and Levi Said, J. 2020, European Physical Journal C, 80, 640
Chaubey, R. and Shukla, A. K. 2013, Ap&SS, 343, 415
Chen, C.-M. and Kao, W. F. 2001, PhRvD, 64, 124019
Clocchiatti, A., Schmidt, B. P., Filippenko, A. V., et al. 2006, ApJ, 642, 1
De Felice, A. and Tsujikawa, S. 2010, Living Reviews in Relativity, 13, 3
Debnath, P. S. and Paul, B. C. 2021, Ap&SS, 366, 32
Dixit, A., Bhardwaj, V. K., Pradhan, A. and Krishnannair, S. 2023a, Indian Journal of Physics, 97, 3695
Dixit, A., Zeyauddin, M. and Pradhan, A. 2023b, European Physical Journal Plus, 138, 1092
Feng, B., Wang, X. and Zhang, X. 2005, PhLB, 607, 35
Ghaderi, K., Shekh, S. H., Karimizadeh, K. and Pradhan, A. 2024, Indian Journal of Physics, 98, 2205
Golchin, H. and Mehdizadeh, M. R. 2019, European Physical Journal C, 79, 777
Harko, T., Lobo, F. S. N., Nojiri, S. and Odintsov, S. D. 2011, PhRvD, 84, 024020
Hinshaw, G., Larson, D., Komatsu, E., et al. 2013, ApJS, 208, 19
Jamil, M., Momeni, D. and Myrzakulov, R. 2013, GReGr, 45, 263
Kamenshchik, A., Moschella, U. and Pasquier, V. 2001, PhLB, 511, 265
Kantowski, R. and Sachs, R. K. 1966, Journal of Mathematical Physics, 7, 443
Kristian, J. and Sachs, R. K. 1966, ApJ, 143, 379
Lee, H. W., Kim, K. Y. and Myung, Y. S. 2011, European Physical Journal C, 71, 1748
Liu, D. and Reboucas, M. J. 2012, PhRvD, 86, 083515
Liu, T., Zhang, X. and Zhao, W. 2018, PhLB, 777, 286
Maurya, D. C., Pradhan, A. and Dixit, A. 2020, International Journal of Geometric Methods in Modern Physics, 17, 2050014
Mishra, B., Tripathy, S. K. and Ray, P. P. 2018, Ap&SS, 363, 86
Moraes, P. H. R. S. and Sahoo, P. K. 2017, PhRvD, 96, 044038
Myrzakulov, N., Shekh, S. H., Pradhan, A. and Dixit, A. 2025, JHEAp, 47, 100374
Nojiri, S. and Odintsov, S. D. 2024, PDU, 46, 101702
Nojiri, S. and Odintsov, S. D. 2025, PDU, 48, 101899
Nojiri, S., Odintsov, S. D. and Oikonomou, V. K. 2016, PhRvD, 93, 084050
Nojiri, S., Odintsov, S. D. and Oikonomou, V. K. 2022, Nuclear Physics B, 980, 115850
Nojiri, S., Odintsov, S. D. and Oikonomou, V. K. 2025, PhRvD, 112, 104035
Odintsov, S. D. and Oikonomou, V. K. 2025a, PhLB, 870, 139907
Odintsov, S. D. and Oikonomou, V. K. 2025b, PhLB, 870, 139909
Peebles, P. J. E. and Ratra, B. 2003, RvMP, 75, 559
Perlmutter, S. et al. 1999, ApJ, 517, 565
Planck Collaboration, Ade, P. A. R., Aghanim, N., et al. 2014, A&A, 571, A16
Pradhan, A. and Jaiswal, R. 2018, International Journal of Geometric Methods in Modern Physics, 15, 1850076
Pradhan, A. and Jotania, K. 2011, Indian Journal of Physics, 85, 497
Pradhan, A., Pandey, P. and Singh, S. K. 2007, International Journal of Theoretical Physics, 46, 1584
Pradhan, A., Dixit, A., Ali, A. and Banerjee, A. 2024a, International Journal of Geometric Methods in Modern Physics, 21, 2450206
Pradhan, A., Dixit, A. and Zeyauddin, M. 2024b, International Journal of Geometric Methods in Modern Physics, 21, 2450027
Rao, V. U. M., Vinutha, T. and Vijaya Santhi, M. 2008, Ap&SS, 314, 213
Rao, V. U. M., Vinutha, T., Neelima, D. and Surya Narayana, G. 2015, Advances in Research on Physics, 10, 0017
Ray, J. R. 1982, Il Nuovo Cimento B, 71, 19
Reddy, D. R. K., Anitha, S. and Umadevi, S. 2016, Ap&SS, 361, 349
Riess, A. G., Filippenko, A. V., Challis, P., et al. 1998, AJ, 116, 1009
Riess, A. G., Strolger, L.-G., Tonry, J., et al. 2004, ApJ,

607, 665
Saha, B., Amirhashchi, H. and Pradhan, A. 2012, Ap&SS, 342, 257
Sahni, V. and Starobinsky, A. 2000, IJMPD, 9, 373
Sahoo, P., Bhattacharjee, S., Tripathy, S. K. and Sahoo, P. K. 2020, MPLA, 35, 2050095
Sahoo, P. K., Mishra, B., Sahoo, P. and Pacif, S. K. J. 2016, European Physical Journal Plus, 131, 333
Sahoo, P. K., Moraes, P. H. R. S., Sahoo, P. and Bishi, B. K. 2018, European Physical Journal C, 78, 736
Santos, J., Alcaniz, J. S., Reboucas, M. J. and Carvalho, F. C. 2007, PhRvD, 76, 083513
Scolnic, D. M., Jones, D. O., Rest, A., et al. 2018, ApJ, 859, 101
Sen, A. 2002, Journal of High Energy Physics, 7, 065
Shabani, H. and Ziaie, A. H. 2018, European Physical Journal C, 78, 397
Sharif, M. and Zubair, M. 2013, Journal of the Physical Society of Japan, 82, 014002
Sharma, U. K., Zia, R., Pradhan, A., et al. 2019, RAA, 19, 055
Shekh, S. H., Mustafa, G., Caliskan, A., et al. 2023a, International Journal of Geometric Methods in Modern Physics, 20, 2350207
Shekh, S. H., Myrzakulov, N., Bouali, A. and Pradhan, A. 2023b, Communications in Theoretical Physics, 75, 095401
Shekh, S. H., Pradhan, A., Dixit, A., et al. 2025, MPLA, 40, 2450187
Singh, A., Mandal, S., Chaubey, R. and Raushan, R. 2025, PDU, 47, 101798
Sotiriou, T. P. and Faraoni, V. 2008, CQGra, 25, 205002
Spergel, D. N., Verde, L., Peiris, H. V., et al. 2003, ApJS, 148, 175
Tegmark, M., Strauss, M. A. and Blanton, M. R. 2004, PhRvD, 69, 103501
Thorne, K. S. 1967, ApJ, 148, 51
Tolman, R. C. 1931, PhRv, 37, 1639
Tonry, J. L., Schmidt, B. P., Barris, B., et al. 2003, ApJ, 594, 1
Tripathy, S. K., Khuntia, R. K. and Parida, P. 2019, European Physical Journal Plus, 134, 504
Tsujikawa, S. 2008, PhRvD, 77, 023507
Verma, S., Dixit, A., Pradhan, A. and Barak, M. S. 2026, JHEAp, 49, 100440
Vijaya Santhi, M., Rao, V. U. M., Gusu, D. M. and Aditya, Y. 2018, International Journal of Geometric Methods in Modern Physics, 15, 1850161
Vinutha, T. and Kavya, K. S. 2020, European Physical Journal Plus, 135, 306
Vinutha, T. and Kavya, K. S. 2022, International Journal of Geometric Methods in Modern Physics, 19, 2250046
Vinutha, T. and Sri Kavya, K. 2021, Results in Physics, 23, 103863
Vinutha, T. and Venkata Vasavi, K. 2021, NewA, 89, 101647
Vinutha, T., Rao, V. U. M., Bekele, G. and Kavya, K. S. 2021a, Indian Journal of Physics, 95, 1933
Vinutha, T., Sri Kavya, K. and Niharika, K. 2021b, PDU, 34, 100896
Vinutha, T., Vasavi, K. V., Niharika, K. and Satyanarayana, G. 2023, Indian Journal of Physics, 97, 1621
Wang, J. and Liao, K. 2012, CQGra, 29, 215016
Wang, J., Wu, Y.-B., Guo, Y.-X., Yang, W.-Q. and Wang, L. 2010, PhLB, 689, 133
Weinberg, S. 1989, RvMP, 61, 1
Yadav, A. K., Sahoo, P. K. and Bhardwaj, V. 2019, MPLA, 34, 1950145
Zhao, G.-B., Xia, J.-Q., Li, H., et al. 2007, PhLB, 648, 8

APPENDIX

$$\chi = \frac{36\zeta(t^2(m^2+m+1)\zeta + \frac{1}{3}m^2 + \frac{1}{2}m + \frac{1}{6}}{(2m+1)^2}$$

$$\eta = \frac{-4(m+\frac{1}{2})^2(e^{\zeta t^2})^{\frac{-6m}{2m+1}} + (108\zeta^2t^2 + 24\zeta)m^2 + 12\zeta m}{(2m+1)^2}$$

$$\beta = \frac{-4(m+\frac{1}{2})^2(e^{\zeta t^2})^{\frac{-6m}{2m+1}} + 36m\zeta^2t^2(m+2)}{(2m+1)^2}$$

$$\phi_1 = \frac{(16\pi + 3\lambda)\cosh(\varrho_1)^2}{2\cosh(\varrho_1)^2 - 2\nu}$$

$$\phi_2 = \frac{\lambda\cosh(\varrho_1)^2}{2\cosh(\varrho_1)^2 - 2\nu}$$

$$\phi_3 = \frac{\nu\gamma\sinh(\varrho_1)\cosh(\frac{1}{(2m+1)^2\gamma}\varrho_1)}{2\cosh(\varrho_1)^2 - 2\nu}$$

$$\phi_4 = \frac{\varrho_2}{(2m+1)^2((e^{\zeta t^2})^{\frac{3m}{2m+1}})^2(-\cosh(\varrho_1)^2+\nu)}$$

$$\phi_5 = \frac{\varrho_3}{(2m+1)^3\gamma((e^{\zeta t^2})^{\frac{3m}{2n+1}})^2\cosh(\varrho_1)(-\cosh(\varrho_1)^2+\nu)}$$

$$\phi_6 = \frac{\phi_5}{m}$$

$$\phi_7 = \frac{\varrho_4}{(2m+1)^3\gamma((e^{\zeta t^2})^{\frac{3m}{2n+1}})^2\cosh(\varrho_1)(-\cosh(\varrho_1)^2+\nu)}$$

$$\phi_8 = \frac{\varrho_5}{(2m+1)^4\gamma^2((e^{\zeta t^2})^{\frac{3m}{2n+1}})^4\cosh(\varrho_1)(-\cosh(\varrho_1)^2+\nu)}$$

$$\varrho_1 = \frac{\varrho_6}{(2m+1)^2\gamma}$$

$$\varrho_2 = 108(((\zeta t^2 + \frac{2}{9})m^2 + (\frac{2\zeta t^2 m}{3} + \frac{2m}{9}) + \frac{\zeta t^2}{3} + \frac{1}{18})\zeta\Big((e^{\zeta t^2})^{\frac{3m}{2n+1}}\Big)^2 - \frac{1}{27}(m+\frac{1}{2})^2)\nu$$

$$\varrho_3 = 5184\zeta^2 m\Big(\zeta(m^2 + \frac{2m}{3} + \frac{1}{3})\Big((e^{\zeta t^2})^{\frac{3m}{2n+1}}\Big)^2 + \frac{m^2}{9} + \frac{m}{18}\Big)\nu t^2\sinh(\varrho_1)$$

$$\varrho_4 = -576\nu\zeta\Big(\frac{-3(m^2+\frac{2m}{3}+\frac{1}{3})\zeta\Big((e^{\zeta t^2})^{\frac{3m}{2n+1}}\Big)^2}{2} + (\zeta t^2 - \frac{1}{6})m^2 - \frac{m}{12}\Big)\sinh(\varrho_1)$$

$$\varrho_5 = 746496t^2\nu\Big(\cosh(\varrho_1)^2 - \frac{3}{2}\Big)\Big(\zeta(m^2 + \frac{2m}{3} + \frac{1}{3})\Big((e^{\zeta t^2})^{\frac{3m}{2n+1}}\Big)^2 + \frac{m^2}{9} + \frac{m}{18}\Big)^2\zeta^2$$

$$\varrho_6 = 8(m+\frac{1}{2})^2(e^{\zeta t^2})^{\frac{-6m}{2m+1}} - 216\zeta(t^2(m^2+\frac{2m}{3}+\frac{1}{3})\zeta + \frac{2(n+\frac{1}{2})^2}{9})$$

$$\chi_1 = \frac{\delta_2}{(m+1)^2}$$

$$\eta_1 = \frac{\delta_3}{(m+1)^2}$$

$$\beta_1 = \frac{\delta_4}{(n+1)^2}$$

$$\epsilon = \frac{-3(m+1)^2e^{-2\zeta t^2} + 8\zeta^2t^2(m^2+4m+1)}{(m+1)^2}$$

$$\iota_1 = \frac{(16\pi+3\lambda)\cosh(\delta_1)^2}{2\cosh(\delta_1)^2 - 2\nu}$$

$$\iota_2 = \frac{\lambda\cosh(\delta_1)^2}{2\cosh(\delta_1)^2 - 2\nu}$$

$$\iota_3 = \frac{\nu\gamma\sinh(\delta_1)\cosh(\delta_1)}{2\cosh(\delta_1)^2 - 2\nu}$$

$$\iota_4 = \frac{\delta_5}{(m+1)^2(-\cosh(\delta_1)^2+\nu)}$$

$$\iota_5 = \frac{\iota_{13}}{(m+1)\iota_{10}}$$

$$\iota_6 = \frac{\iota_5}{m}$$

$$\iota_7 = \frac{\iota_{12}}{\iota_{10}}$$

$$\iota_8 = \frac{\delta_6}{(m+1)^4\gamma^2\cosh(\delta_1)^2(-\cosh(\delta_1)^2+\nu)}$$

$$\iota_9 = \frac{\iota_{11}}{\iota_{10}}$$

$$\iota_{10} = (m+1)^2\gamma\cosh(\delta_1)(-\cosh(\delta_1)^2+\nu)$$

$$\iota_{11} = 448e^{-2\zeta t^2}\nu\zeta^2\Big(\zeta(m^2+\frac{10m}{7}+1)e^{2\zeta t^2} + \frac{3(m+1)^2}{14}\Big)\sinh(\delta_1)t^2$$

$$\iota_{12} = -192e^{-2\zeta t^2}\,\nu\,\sinh(\delta_1)\left(\frac{-7\zeta\left(m^2+\frac{10m}{7}+1\right)e^{2\zeta t^2}}{6} + (\zeta t^2 - \frac{1}{4})(m+1)^2\right)\zeta$$

$$\iota_{13} = 896e^{-2\zeta t^2}\,\nu\,t^2\sinh(\delta_1)\,m\zeta^2\left(\zeta\left(m^2+\frac{10m}{7}+1\right)e^{2\zeta t^2} + \frac{3(m+1)^2}{14}\right)$$

$$\delta_1 = \frac{6(m+1)^2e^{-2\zeta t^2}}{(m+1)^2\gamma} \times \frac{-56\Big((t^2(m^2+\frac{10}{7}m+1)\zeta + \frac{3(m+1)^2}{14})\Big)\zeta}{(m+1)^2\gamma}$$

$$\delta_2 = -(m+1)^2e^{-2\zeta t^2} + (16\zeta^2t^2+4\zeta)m^2 + (16\zeta^2t^2+8\zeta)m + 16\zeta^2t^2 + 4\zeta$$

$$\delta_3 = (4(((\zeta t^2+\frac{1}{2})m^2 + (4\zeta t^2+2)m + 7\zeta t^2 + \frac{3}{2})\xi e^{2\zeta t^2} - \frac{(m+1)^2}{4}))e^{-2\zeta t^2}$$

$$\delta_4 = 28e^{-2\zeta t^2}(((\zeta t^2+\frac{3}{14})m^2 + (\frac{4\zeta t^2}{7}+\frac{2}{7})m + \frac{\zeta t^2}{7}+\frac{1}{14})\zeta e^{2\zeta t^2} - \frac{(m+1)^2}{28})$$

$$\delta_5 = 28(((\zeta t^2+\frac{3}{14})m^2 + (\frac{10\zeta t^2}{7}+\frac{3}{7})m + \zeta t^2 + \frac{3}{14})\zeta e^{2\zeta t^2} - \frac{3(m+1)^2}{28})\nu e^{-2\zeta t^2}$$

$$\delta_6 = 50176e^{-4\zeta t^2}\nu\zeta^2(\cosh(\delta_1)^2 - \frac{3}{2})t^2\Big(\zeta(m^2 + \frac{10m}{7}+1)e^{2\zeta t^2} + \frac{3(m+1)^2}{14}\Big)^2$$

$$\chi_2 = \frac{4(m+\frac{1}{2})^2(e^{\zeta t^2})^{\frac{-6}{2m+1}} + (108\zeta^2t^2+24\zeta)m^2 + 12m\zeta}{(2m+1)^2}$$

$$\eta_2 = \frac{\xi_2}{(2m+1)^2}$$

$$\beta_2 = \frac{-4(m+\frac{1}{2})^2(e^{\zeta t^2})^{\frac{-6}{2m+1}} + 36\zeta^2t^2m(m+2)}{(2m+1)^2}$$

$$\alpha_1 = \frac{(16\pi+3\lambda)\cosh(\xi_1)^2}{2\cosh(\varrho_1)^2 - 2\nu}$$

$$\alpha_2 = \frac{\lambda\cosh(\xi_1)^2}{2\cosh(\xi_1)^2 - 2\nu}$$

$$\alpha_3 = \frac{\nu\gamma\sinh(\xi_1)\cosh(\xi_1)}{2\cosh(\xi_1)^2 - 2\nu}$$

$$\alpha_4 = \frac{\xi_3}{(2m+1)^2((e^{\zeta t^2})^{\frac{3}{2m+1}})^2(-\cosh(\xi_1)^2+\nu)}$$

$$\alpha_5 = \frac{\xi_4}{(2m+1)^3\gamma((e^{\zeta t^2})^{\frac{3}{2m+1}})^2(-\cosh(\xi_1)^2+\nu)\cosh(\xi_1)}$$

$$\alpha_6 = \frac{\xi_5}{(2m+1)^2\gamma((e^{\zeta t^2})^{\frac{3}{2m+1}})^2(-\cosh(\xi_1)^2+\nu)\cosh(\xi_1)}$$

$$\alpha_7 = \frac{\xi_6}{(2m+1)^4\gamma^2((e^{\zeta t^2})^{\frac{3}{2m+1}})^4(-\cosh(\xi_1)^2+\nu)\cosh(\xi_1)^2}$$

$$\alpha_8 = \frac{\xi_7}{(2m+1)^3\gamma^2((e^{\zeta t^2})^{\frac{3}{2m+1}})^2(-\cosh(\xi_1)^2+\nu)^{\cosh(\xi_1)}}$$

$$\xi_1 = \frac{\xi_8}{(2m+1)^2\gamma}$$

$$\xi_2 = -4(m+\frac{1}{2})^2(e^{\zeta t^2})^{\frac{-6}{2m+1}} + (36\zeta^2t^2+12\zeta)m^2 + (36\zeta^2t^2+18\zeta)m + 36\zeta^2t^2 + 6\zeta$$

$$\xi_3 = 108(((\zeta t^2+\frac{2}{9})m^2 + (\frac{2\zeta t^2m}{3}+\frac{2m}{9}) + \frac{\zeta t^2}{3}+\frac{1}{18})\zeta((e^{\zeta t^2})^{\frac{3}{2m+1}})^2 - \frac{1}{27}(m+\frac{1}{2})^2)\nu$$

$$\xi_4 = 5184\zeta^2\sinh(\xi_1)mt^2\nu\Big(\zeta(m^2+\frac{2m}{3}+\frac{1}{3})\big((e^{\zeta t^2})^{\frac{3}{2m+1}}\big)^2 + \frac{m}{9}+\frac{1}{18}\Big)$$

$$\xi_5 = 864\zeta \sinh(\xi_1)\nu\Big(\zeta(m^2+\frac{2m}{3}+\frac{1}{3})((e^{\zeta t^2})^{\frac{3}{2m+1}})^2 - \frac{2\zeta t^2}{3}+\frac{m}{9}+\frac{1}{18}\Big)$$

$$\xi_6 = 746496\nu t^2\Big(\zeta(m^2+\frac{2m}{3}+\frac{1}{3})((e^{\zeta t^2})^{\frac{3}{2m+1}})^2+\frac{m}{9} + \frac{1}{18}\Big)^2\zeta^2(\cosh(\xi_1)^2-\frac{3}{2})$$

$$\xi_7 = 5184\nu t^2\Big(\zeta(m^2+\frac{2m}{3}+\frac{1}{3})((e^{\zeta t^2})^{\frac{3}{2m+1}})^2+\frac{m}{9} + \frac{1}{18}\Big)\zeta^2\sinh(\xi_1)$$

$$\xi_8 = 8(m+\frac{1}{2})^2(e^{\zeta t^2})^{\frac{-6}{2m+1}} - 216\zeta(t^2(m^2+\frac{2m}{3}+\frac{1}{3})\zeta + \frac{2(n+\frac{1}{2})^2}{9})$$

ПРОУЧАВАЊЕ АНИЗОТРОПНИХ ЦИКЛИЧНИХ КОСМОЛОШКИХ МОДЕЛА У МОДИФИКОВАНОЈ ГРАВИТАЦИЈИ

T. Vinutha[1], K. Niharika[2] and K. Sri Kavya[3]

[1] *Dept. of Applied Mathematics, AUCST, Andhra University, Visakhapatnam-530003, India*
E–mail: *vinuthatummala@gmail.com*

[2] *Dept. of Mathematics, Vignan's Institute of Information Technology(Autonomous), Visakhapatnam-530049, India*

[3] *Dept. of Mathematics, Maharaj Vijayaram Gajapathi Raj College of Engineering, Vizianagaram-535005, India*

УДК 524.8 : 524.882 : 530.12
Оригинални научни рад

Циљ овог рада је истраживање анизотропних цикличних (тзв. "*bouncy*") космолошких модела Бијанкијевог типа - III, V и VI_0 - у оквиру модификоване гравитације. Ова студија се бави испитивањем $f(R,T)$ гравитације, односно $f_1(R)+f_2(T) = R-\nu\gamma\tanh(R/\gamma)+\lambda T$ где су ν, γ и λ константе, R Ричијев скалар, а T траг тензора енергије и импулса. За решавање једначина поља ова три модела разматрају се две претпоставке: i) скалар експанзије је пропорционалан скалару смицања, и ii) фактор скалирања је цикличан. У овом раду циклични фактор скалирања проучаван је у експоненцијалном облику (тј. као симетрично одбијање), а резултујући графици показују да фаза контракције одражава фазу експанзије. Поједини параметри сва три модела су анализирани, а њихов утицај приказан је графички. Енергетски услови су испитивани у контексту $f(R,T)$ гравитације, а резултати указују на нарушавање нултог и јаког енергетског услова док је доминантни енергетски услов задовољен, што указује на сценарио убрзаног ширења Универзума. Стабилност добијеног модела испитана је применом технике пертурбација. Овај рад дао је занимљиве резултате који подржавају савремена посматрања космоса.